Reduced scale model testing for prediction of eigenfrequencies and hydro-acoustic resonances in hydropower plants operating in off-design conditions

A Favrel[1], **J Gomes Pereira Junior**[1], **C Landry**[2], **S Alligné**[2], **C Nicolet**[2], **F Avellan**[1]

[1] Ecole Polytechnique Fédérale de Lausanne, Avenue de Cour 33bis, Lausanne, Switzerland
[2] Power Vision Engineering Sàrl, Ecublens, Switzerland

email: arthur.favrel@epfl.ch

Abstract. The increasing share of renewable energy sources for the electricity supply, such as wind and solar, pushes the operators to extend hydropower plant units operating range to meet the transmission system operator requirements. However, in off-design operating conditions, flow instabilities are developing in Francis turbines, inducing cavitation, pressure pulsations and potentially resonance that can threaten the stability of the whole system. Reduced scale model testing is commonly performed to assess the hydraulic behaviour of the machine for industrial projects. However, pressure pulsations and resonance conditions cannot be directly transposed from model to prototype since the eigenfrequencies of the system depend on both the cavitation volume and the characteristics of the hydraulic circuit, which are different from model to prototype. In this paper, a methodology developed in the framework of the HYPERBOLE European research project for predicting the eigenfrequencies of hydropower plant units operating in off-design conditions is introduced. It is based on reduced scale model testing and proper one-dimensional modelling of the hydraulic circuits, including the draft tube cavitation flow, at both the model and prototype scales. The hydro-acoustic parameters in the draft tube are identified at the model scale for a wide number of operating conditions and, then, transposed to the full-scale machine, together with the precession frequency for part load conditions. This enables the prediction of the eigenfrequencies and resonance conditions of the full-scale generating unit.

1. Introduction

Hydraulic turbines operating in off-design conditions experiences the development of unfavourable flow patterns inducing cavitation and pressure fluctuations, which can lead to output power swings [1] and mechanical vibrations reducing the life expectancy of the machine [2].

In the case of Francis turbines operating in part load conditions, i.e. with a discharge value lower than the value at the Best Efficiency Point (BEP), a cavitation vortex rope is developing at the runner outlet in the draft tube. Its periodical motion of precession with a frequency comprised between 0.2 and 0.4 times the runner frequency [3] acts as a pressure excitation source, leading to the propagation of pressure pulsations in the whole system [4] at the same frequency. Hydro-acoustic resonance might be observed in case of matching between the precession frequency of the vortex and one of the eigenfrequencies of the hydraulic circuit [5] [6]. It induces a dramatic amplification of the pressure pulsations and output power surges that can put at risk the stability of the hydro-mechanical system and

of the electrical transmission system in the worst case. In full load conditions, i.e. with a discharge value higher than the value at the BEP, an axisymmetric cavitation vortex developing along the draft tube cone centreline can enter self-oscillations under certain conditions, inducing severe pressure pulsations in the whole hydraulic circuit [7] [8].

The accurate assessment of the stability of hydropower plants and the prediction of resonance conditions is crucial to ensure a safe extension of their operating range without unnecessary restrictions. For hydropower projects, experimental tests are commonly performed on reduced scale physical models enabling the prediction of the hydraulic behaviour of the prototype machine in terms of efficiency and cavitation with an excellent confidence level. However, although both geometric homology and kinematic similarity between model and prototype scales are fulfilled according to the IEC International Standard [9], the amplitude of pressure fluctuations cannot be directly transposed from the model to the prototype as the eigenfrequency values of the system depend on both the cavitation volume and the characteristics of the hydraulic circuit. To predict and simulate resonance conditions, one-dimensional (1D) hydro-acoustic models including the draft tube cavitation flow have therefore been developed by Dörfler [4], Couston and Philibert [10] and more recently Alligné et al. [11].

Alligné et al. [12] predicted the first eigenfrequency of a hydropower generating unit at two different part load operating points by transposing the hydro-acoustic parameters of the draft tube cavitation flow identified on the reduced scale model by Landry et al. [13]. In the present study, a methodology to predict eigenfrequencies of hydropower plant units operating at both part load and full load is proposed and validated. The methodology is based on reduced scale physical model tests and 1D models of both the test rig at the model scale and the full-scale generating unit. The methodology is applied at part load conditions and enables the prediction of resonance conditions. At full load, it enables the prediction of the instability frequency, since the vortex rope enters self-oscillations at one of the first eigenfrequencies of the hydraulic circuit.

2. Reduced scale physical model test

The test case is a 1:16 reduced scale physical model of a Francis turbine featuring a 16-blades runner and a specific speed of $\nu = 0.27$, see Figure 1. The present test case has been extensively investigated at deep part load [14], part load [15] and full load conditions [16]. The reduced scale physical model is installed on the PF3 closed-loop test rig of the EPFL Laboratory for Hydraulic Machines. The test rig features two axial double-volute pumps of 400 kW to generate the specified head by adjusting the pumps speed while the discharge is adjusted by changing the opening angle of the guide vanes. The turbine shaft is connected to a generator that enables the control of the runner speed. The test rig allows for accurate performance tests of the reduced scale model of hydraulic machines within an accuracy better than 0.3 % according to the IEC International Standard [9]. Wall flush-mounted piezo-resistive pressure transducers are placed in the model to measure the absolute wall pressure. A set of 4 pressure sensors regularly spaced by 90° is placed in a horizontal cross-section of the draft tube cone located $0.39 \times D$ downstream the runner outlet, with D the outlet runner diameter. This enables the decomposition of the pressure fluctuations into convective and synchronous components [17]. Two additional pressure sensors, p_5 and p_6, are installed in the high pressure connecting pipe of the machine to directly measure the synchronous pressure component and to evaluate the hydro-acoustic response of the system.

At both part and full loads, pressure fluctuations measurements are performed within a wide range of discharge factor values for 4 different values of speed factor while the net head H and the Froude number $\mathrm{F} = (H / D)^{0.5}$ are kept constant. The measurements are performed for a value of Thoma number σ_{rated} corresponding to the average *NPSE*-value on the prototype. In addition, measurements in Froude similitude, i.e. with a Froude number corresponding to the value on the prototype, are also performed for several operating conditions. The investigated operating conditions are summarized in Figure 2.

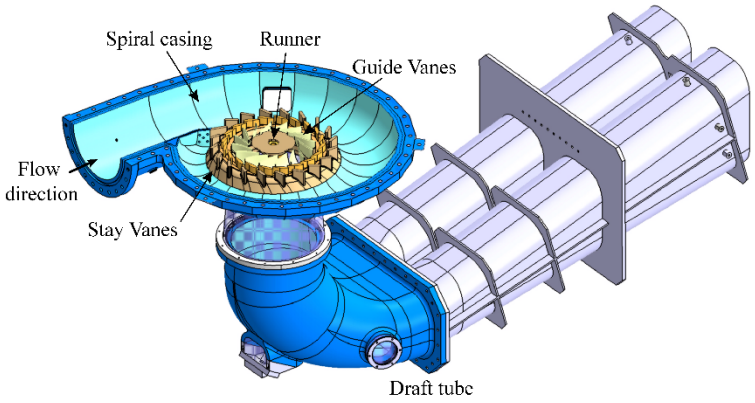

Figure 1. 3D view of the reduced scale physical model of a Francis turbine used for the present investigation.

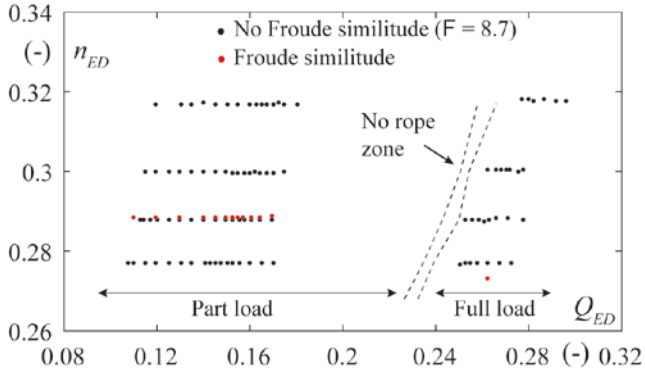

Figure 2. Investigated operating conditions.

3. Experimental identification of the frequencies of interest during model tests

3.1. Identification of the precession frequency and first eigenfrequency at part load conditions

For a given operating point at part load, the precession frequency of the vortex rope and the first eigenfrequency of the test rig can be identified by simple cross-spectral analysis of pressure signals measured in the same cross-section of the draft tube cone, as highlighted by Favrel et al. [18]. Both frequencies are identified for all the investigated operating points at part load.

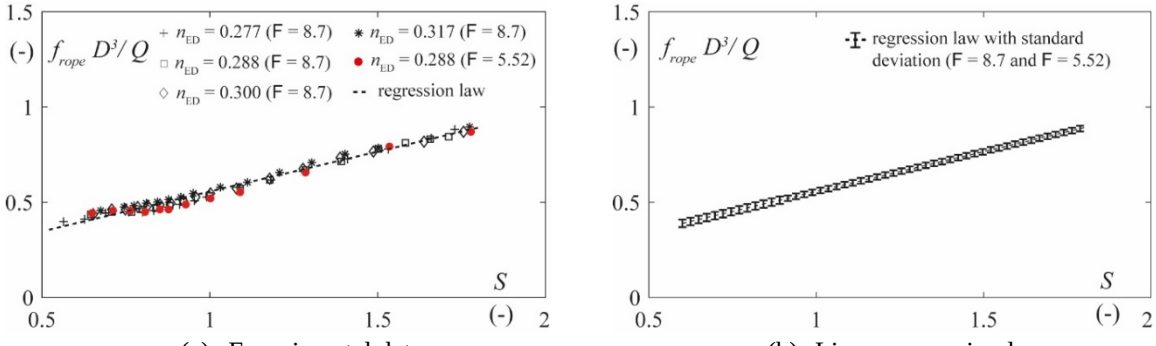

(a) Experimental data (b) Linear regression law

Figure 3. Strouhal number of the precession frequency as a function of the swirl number *S* computed according to [18] at part load conditions.

Both speed and discharge factors influence the value of the precession frequency and the eigenfrequencies of the test rig. However, Favrel et al. [18] showed that the influence of both parameters can be represented by a single curve if the frequencies are plotted as a function of the swirl number, whose analytical expression as a function of the speed and discharge factors was derived [18].

The Strouhal number of the precession frequency is plotted as a function of the swirl number in Figure 3a. All the data, whatever the value of the speed factor and Froude number, collapse to one single curve, which can be represented by a linear regression law with corresponding standard deviation as given in Figure 3b. This curve can be therefore used to determine the precession frequency of the vortex on the complete operating range of the machine at part load, whatever the value of the Froude number.

The first eigenfrequency is also plotted as a function of the swirl number in Figure 4. The data with F = 8.7, i.e. without Froude similitude between prototype and model, collapse to one single curve, which can be represented by a power regression law with corresponding standard deviation as shown in Figure 4b. However, as shown in Figure 4a, the data at F = 5.52 draw a similar curve but with a slight shift, which highlights the influence of the Froude number on the eigenfrequencies of the test rig. In Section 4.2, the value of the first eigenfrequency is used to determine the hydro-acoustic parameters modelling the draft tube cavitation flow.

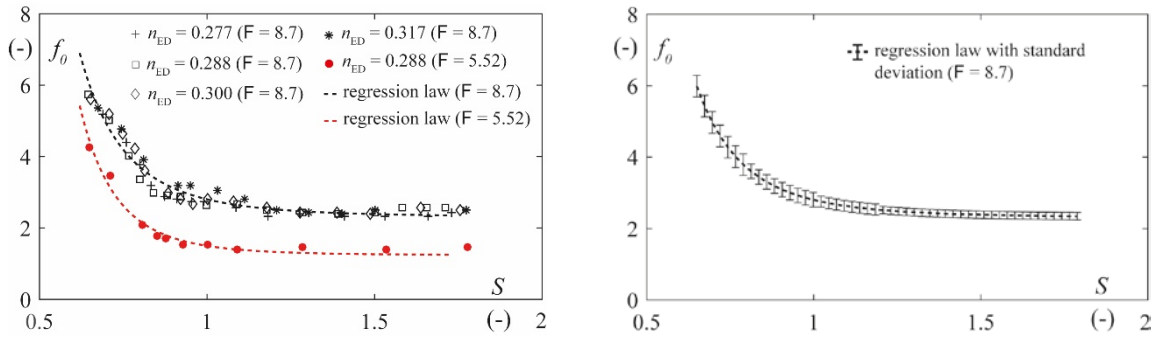

(a) Experimental data (b) Power regression law

Figure 4. First eigenfrequency of the hydraulic circuit as a function of the swirl number at part load.

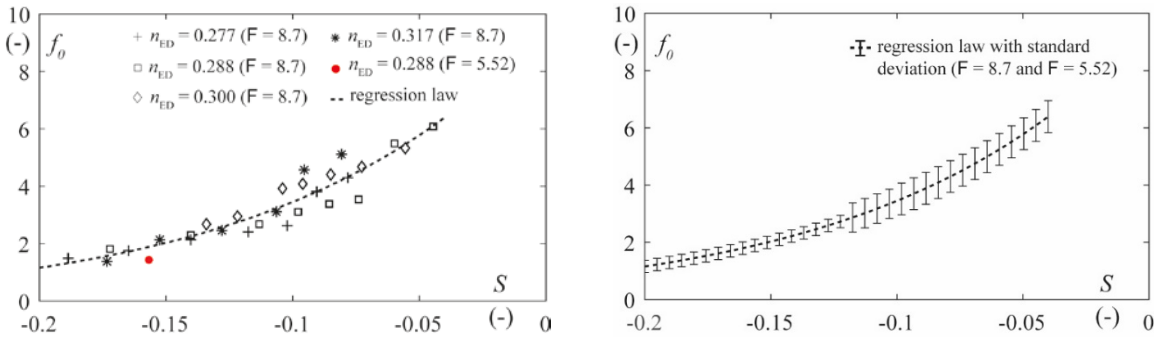

(a) Experimental data (b) Power regression law

Figure 5. First eigenfrequency of the hydraulic circuit as a function of the swirl number at full load.

3.2. Identification of the first eigenfrequency at full load conditions

At full load, the vortex rope enters self-oscillations at the first eigenfrequency of the test rig under certain conditions of pressure level in the draft tube. Therefore, if the vortex rope is unstable, the first eigenfrequency of the test rig can be easily identified by spectral analysis of pressure fluctuations measured in the draft tube cone. The first eigenfrequency of the test rig is determined for all the investigated unstable operating points and plotted as a function of the swirl number in Figure 5a. Once again, all the data, including the one in Froude similitude, collapse to one single curve, whose power regression law with corresponding standard deviation is given in Figure 5b.

4. Identification of hydro-acoustic parameters modelling the draft tube flow at the model scale

In the following, the hydro-acoustic parameters modelling the draft tube cavitation flow are determined for all the investigated operating points by using the value of the first eigenfrequency and a 1D hydro-

acoustic model of the test rig. First, a brief description of the hydro-acoustic modelling of the draft tube cavitation flow is provided.

4.1. Hydro-acoustic modelling of draft tube cavitation flow

Numerical models of both the test rig at the model scale and the hydropower plant generating unit are established with the SIMSEN software [19]. The cavitation vortex rope developing in Francis turbines draft tube operating in off-design conditions must be properly modelled to take into account the additional compressibility and dissipation induced by the presence of a gaseous volume in the draft tube. In the following, the numerical model developed by Alligné et al. [11] is used to take also into account the divergent geometry of the draft tube and the convective terms of the momentum equation. All the terms are already extensively introduced and explained in Alligné et al. [11] and Landry et al. [13]. In particular, an additional dissipation is introduced and represented in the electrical T-shaped circuit by a hydraulic resistance R_μ to take into account the internal processes breaking the thermodynamic equilibrium between the cavitation volume and the surrounding liquid:

$$R_\mu = \frac{\mu''}{\rho_w g A \mathrm{d}x} \tag{1}$$

where μ'' is the bulk viscosity, ρ_w is the water density, A and dx are the section and the length of the pipe element, respectively, and g is the gravity acceleration.

The additional compressibility introduced by the presence of a cavitation volume in the draft tube is modelled by the cavitation compliance Cc, introduced first by Brennen and Acosta [20], which represents the variation of the cavitation volume with respect to the pressure:

$$Cc = -\frac{\partial V}{\partial h} \tag{2}$$

where h is the piezometric head. The equivalent compliance C_{eq} of the draft tube, including the wall, the water and the cavitation volume, implicitly defines the local wave speed a in the draft tube and is expressed as follows:

$$C_{eq} = (1-\beta)\times C_0 + Cc = \frac{gA\mathrm{d}x}{a^2} \tag{3}$$

where β is the void fraction, i.e. the ration between the cavitation volume and the total volume of the draft tube, and C_0 is the compliance of the draft tube without cavitation. In cavitation conditions, the compressibility of both the draft tube wall and the water volume is negligible compared with the one of the cavitation volume, which finally leads to:

$$Cc \approx \frac{gA\mathrm{d}x}{a^2} \tag{4}$$

The precession of the vortex rope acts also as a momentum excitation source, yielding the propagation of synchronous pressure pulsations in the whole hydraulic circuit. It is taken into account in the 1D numerical model of the draft tube cavitation flow by introducing an additional momentum source S_h. Finally, the unknown parameters in the 1D representation of the cavitation vortex rope are the bulk viscosity μ'', the local wave speed a and the local momentum excitation source S_h. However, the present study focuses only on the identification of the wave speed and the bulk viscosity since the excitation source is not linked with the eigenfrequencies of the hydraulic circuit.

4.2. Identification of hydro-acoustic parameters based on the value of the first eigenfrequency

During a first experimental campaign with the same test case, Landry et al. [13] identified the wave speed and the bulk viscosity for a wide number of part load operating points by using an external

excitation system injecting periodical discharge pulsations into the test rig. By identifying the first eigenfrequency of the test rig and its hydro-acoustic response, the wave speed and the bulk viscosity can be simultaneously calibrated in the 1D model of the test rig considering a distributed cavitation compliance in the Francis turbine draft tube. Landry et al. [13] defined two dimensionless numbers, the dimensionless wave speed Π and the dimensionless bulk viscosity M", as follows:

$$\Pi = \frac{\rho_w a^2}{p_{cone} - p_v} \tag{5}$$

$$\mathrm{M}" = \frac{\mu" f_0}{p_{cone} - p_v} \tag{6}$$

where p_{cone} is the mean pressure in a reference section of the draft tube cone and f_0 is the first eigenfrequency of the hydraulic circuit. It was demonstrated that the relation between these dimensionless parameters and the void fraction β in the draft tube can be approximated by single power functions that are valid whatever the value of speed factor, discharge factor, Thoma number and Froude number. In the present study, no excitation system is used and only the value of the first eigenfrequency is known for a given operating point. To identify the wave speed and the bulk viscosity, a procedure coupling the 1D model of the test rig and the dimensionless law $\Pi = f(\beta)$ and $\mathrm{M}" = f(\beta)$ defined in [13] is used, see [21] for more details.

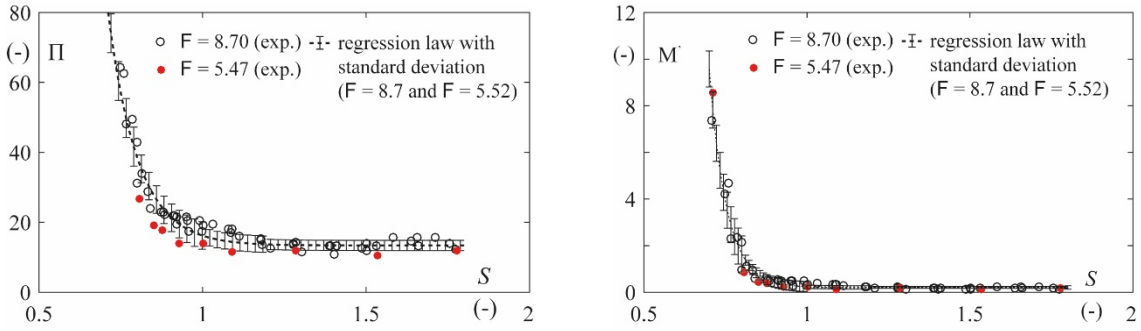

(a) Dimensionless wave speed (b) Dimensionless bulk viscosity

Figure 6. Dimensionless hydro-acoustic parameters as a function of the swirl number at part load.

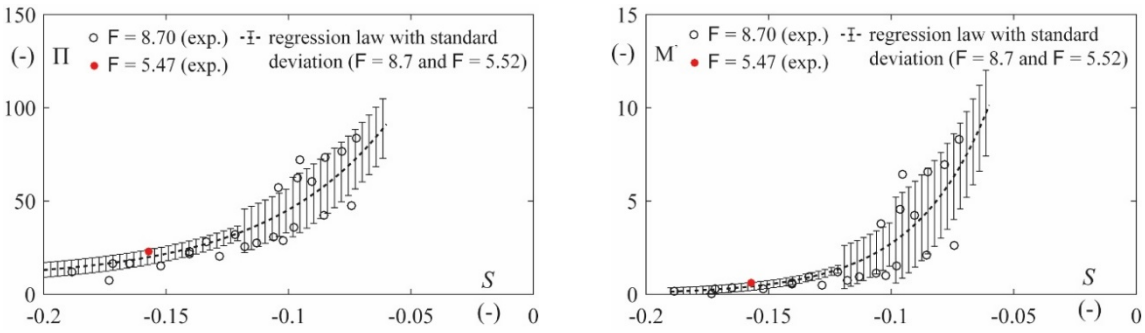

(a) Dimensionless wave speed (b) Dimensionless bulk viscosity

Figure 7. Dimensionless hydro-acoustic parameters as a function of the swirl number at full load.

The dimensionless hydro-acoustic parameters, as defined by Equation 5 and Equation 6, are determined at both part load and full load for all the investigated operating points. The results are plotted as a function of the swirl number at part load and full load in Figure 6 and Figure 7, respectively. At part load, the data collapse to one single curve, whatever the value of the Froude number, for both dimensionless wave speed and bulk viscosity. The resulting curves can be represented by regression

power laws with the corresponding standard deviation. Therefore, these dimensionless laws represent the influence of the speed factor, discharge factor and Froude number on the dimensionless hydro-acoustic parameters for a given Thoma number. Similar behaviour is found at full load, see Figure 7, with however a higher standard deviation for the values of swirl number between S = -0.12 and S = -0.06. Indeed, this operating regime corresponds to the onset of the full load instability, which is very sensitive to operating conditions and can vary because of different gas rates in the water for instance.

5. Prediction of eigenfrequencies at the prototype scale and validation by on-site tests

5.1. On-site tests for validation

On-site tests are performed on the corresponding Francis turbine generating unit, located in Canada and featuring a rated output power of P_{rated} = 444 MW.

Table 1. Investigated operating conditions during prototype tests.

OP	P / P_{rated} (-)	n_{ED} (-)	Q_{ED} (-)	F (-)	σ (-)	S (-)	Comment
1	1.07	0.2787	0.2533	5.72	0.1176	-0.09	Full load
2	0.70	0.2763	0.1632	5.77	0.1021	0.64	Part load
3	0.66	0.2763	0.1556	5.77	0.1024	0.75	Part load
4	0.61	0.2764	0.1439	5.76	0.1038	0.92	Part load
5	0.59	0.2765	0.1406	5.76	0.1045	0.98	Part load
6	0.57	0.2764	0.1361	5.76	0.1036	1.06	Part load
7	0.54	0.2763	0.1302	5.76	0.1033	1.17	Part load
8	0.51	0.2763	0.1237	5.76	0.1036	1.31	Part load
9	0.48	0.2759	0.1188	5.77	0.1008	1.42	Part load

Extensive tests are performed on the generating unit, including stress and pressure measurements on the runner blades and pressure measurements in the draft tube cone, the spiral case and the penstock. The output power of the generating unit is varied from 1.07 % to 48 % of P_{rated} by changing the guide vane opening angle α. The unit is stabilized at 9 different values of output power during several minutes. Output electrical power P, headwater level HWEL, tailwater level TWEL and opening angle of the guide vanes α are measured during the tests. Models for the losses, turbine efficiency and generator efficiency are then used to estimate the corresponding operating points. An explicit model of the turbine efficiency η_h as a function of the discharge Q and the net head H_{net} is built with a data set gathered during the model testing campaign by using the Hermite Polynomials approach described in Andolfatto et al. [22]. The corresponding operating parameters are given in Table 1.

5.2. Transposition of the hydro-acoustic parameters from model to prototype

For each operating point measured on the prototype, the corresponding swirl number is computed by using the analytical expression derived in [18]. The corresponding dimensionless hydro-acoustic parameters can be determined by using the dimensionless laws defined in Figure 6 and Figure 7. By knowing the pressure level in the cone, which is measured by 3 pressure sensors located in the same cross-section of the cone, the wave speed at the prototype scale can be directly computed. However, the transposition of the bulk viscosity requires the value of the first eigenfrequency, see Equation 6. Therefore, the value of the bulk viscosity, together with the first eigenfrequency of the prototype, must be computed by using the algorithm given in Figure 8.

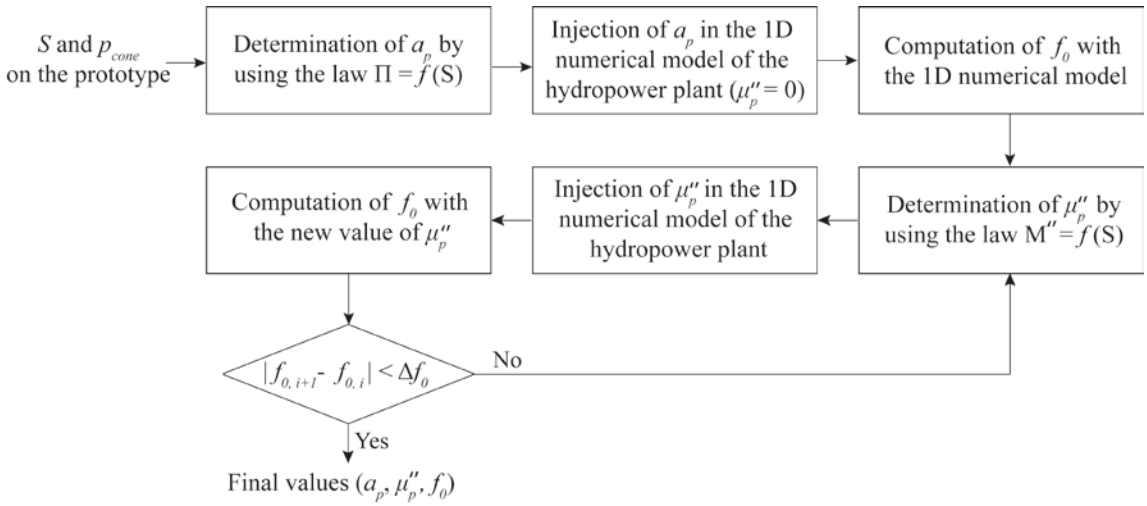

Figure 8. Procedure for computation of the bulk viscosity and the first eigenfrequency at the prototype scale for a given operating point.

5.3. Prediction of resonance at part load conditions

At part load conditions, the precession frequency of the vortex can be predicted at the prototype scale by transposing directly the empirical law defined at the model scale and given in Figure 3b. The first eigenfrequency of the hydropower generating unit is predicted for the operating points tested during on-site measurements by using the procedure described in the previous section. The predicted values of frequency, together with the values identified during on-site tests, are given in Figure 9. It is worth to precise that the first eigenfrequency of the hydropower generating unit can be identified during on-site tests by performing simple spectral analysis of pressure fluctuations measured in the draft tube cone, similarly to model tests.

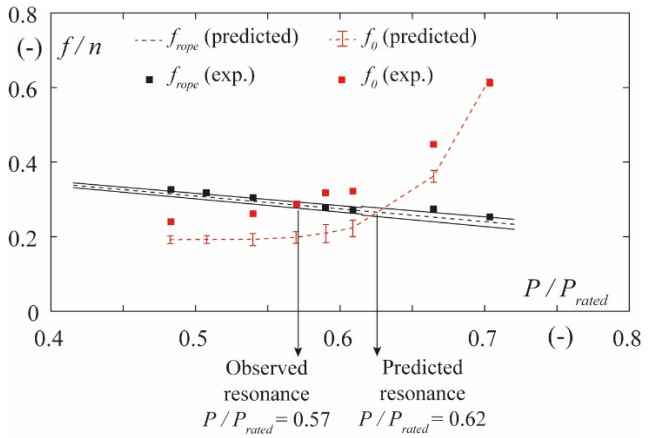

Figure 9. Comparison between predicted and measured frequencies at the prototype scale in part load conditions.

For the precession frequency, the predicted and experimental results are in very good agreement. The highest deviation is observed at $P = 0.66 \times P_{rated}$ and is equal to $0.02 \times n$, which represents 9 % of the predicted value. All the other experimental values are in the range of uncertainty of the predicted values.

For the first eigenfrequency of the prototype, the predicted values feature similar shape to the experimental ones. However, a clear discrepancy is observed between the experimental and predicted results. The difference ranges from $0.01 \times n$ at $P = 0.70 \times P_{rated}$ to $0.11 \times n$ at $P = 0.59 \times P_{rated}$, which corresponds to 2 % and 33 % of the predicted values, respectively. As shown in Figure 9, the resonance is observed during on-site tests at $P \approx 0.57 \times P_{rated}$ whereas the methodology predicts the occurrence of resonance at $P \approx 0.62 \times P_{rated}$, which corresponds to a shift equal to 5 % of the rated output power of the machine. However, it is observed that similitude in terms of pressure conditions in the draft tube cone

between prototype and model for a given part load operating point is not fulfilled for this case study even if Thoma numbers are similar. This might induce discrepancy in terms of local wave speed in the draft tube cone and explain the shift between predicted and experimental values.

5.4. Prediction of full load instability frequency

Only one operating point at full load is investigated during on-site tests. At this point, the cavitation vortex rope enters self-oscillations, leading to strong pressure pulsations in the whole hydraulic circuit of the generating unit, as reported in [8]. The frequency of the instability is determined by spectral analysis of the pressure fluctuations and is equal to $f_0 / n = 0.37$.

The first eigenfrequency of the generating unit, which corresponds to the frequency of the instability, is predicted for this operating point by using the methodology presented previously. The predicted value is equal to $f_0 / n = 0.33 \pm 0.06$. Contrary to the results at part load, the predicted value is in very good agreement with the experimental one: the latter is comprised within the range of uncertainty of the predicted value.

6. Conclusion and discussion

A new methodology for predicting the first eigenfrequency of hydropower plant units with a conventional Francis turbine operating at part load and full load, as well as the precession frequency of the vortex rope at part load, is introduced.

The prediction of the first eigenfrequency of the prototype is based on the experimental identification of the hydro-acoustic parameters modelling the draft tube cavitation flow on the corresponding reduced scale physical model and 1D numerical models of both the test rig at the model scale and the hydropower plant unit. By defining empirical laws linking dimensionless hydro-acoustic parameters and the swirl number, their value can be predicted on the complete operating range of the machine, whatever the value of discharge factor, speed factor and Froude number. Such empirical laws are however valid for one given value of Thoma number. In addition, the precession frequency is expressed at the model scale as a function of the swirl number, which allows representing the influence of both the discharge and speed factors on its value, whatever the Froude number, by a simple linear regression law. The latter is directly transposed from the model to the prototype scale, which enables the prediction of its value on the complete part load operating range of the prototype.

At part load, a perfect agreement is found for the precession frequency between the predicted values and the values identified during on-site tests, which confirms that the precession frequency can be directly transposed from the model to the prototype. For the first eigenfrequency of the prototype, a discrepancy is observed between predicted and experimental values. However, similitude in terms of pressure conditions in the draft tube cone between prototype and model for a given operating point is not fulfilled for this case study even if Thoma numbers are similar, which might induce discrepancy in terms of local wave speed in the draft tube cone. On the contrary, a good agreement is observed at full load between predicted and observed values of the first eigenfrequency of the prototype.

The proposed methodology represents an important milestone for the stability assessment of conventional Francis turbine units operating in off-design conditions and might lead in the future to the revision of the scale-up relating to oscillating phenomena in the IEC 60193 Standard for industrial model testing. Further investigation must focus on the prediction of eigenfrequencies for different *NPSE*-values by using a local cavitation coefficient instead of the Thoma number to ensure similar pressure conditions in the draft tube between model and prototype.

Acknowledgments

The research leading to the results published in this paper is part of the HYPERBOLE research project, granted by the European Commission (ERC/FP7-ENERGY-2013-1-Grant 608532). The authors would like to thank BC Hydro (CA) for making available the reduced scale model, in particular Danny Burggraeve and Jacob Iosfin. Moreover, the authors would like to acknowledge the commitment of the

Laboratory for Hydraulic Machines' technical staff, especially Raymond Fazan, Georges Crittin, Alain Renaud and Vincent Berruex, and the HYPERBOLE partners involved in the on-site tests.

References

[1] Rheingans W 1940 *Transactions of the ASME* **62** 171-184
[2] Lowys P, Andre F, Ferreira da Silva A, Duarte F and Payre J.-P 2014 *Proceedings of Hydrovision, Nashville, USA*
[3] Arpe J, Nicolet C and Avellan F 2009 *Journal of Fluids Engineering* **131**(8) 081102
[4] Dörfler P 1982 *Proceedings of the 11th IAHR Symposium on Operating Problem of Pump Stations and Powerplants, Amsterdam, Netherlands*
[5] Favrel A, Landry C, Müller A, Yamamoto K and Avellan F 2014 *IOP Conference Series: Earth and Environmental Science* **22** 032035
[6] Fritsch A and Maria D 1988 *Houille Blanche* **3**(3-4) 273-281
[7] Müller A, Favrel A, Landry C and Avellan F 2017 *Journal of Fluids and Structures* **69** 56-71
[8] Valentin D, Presas A, Egusquiza E, Valero C, Egusquiza M and Bossio M 2017 *Energies* **10** 2124
[9] IEC Standards, 60193: hydraulic turbines, storage pumps and pump-turbines - model acceptance tests (second edition) 1999 International Commission
[10] Couston M and Philibert R 1998 *The International Journal on Hydropower and Dams* **1** 146-158
[11] Alligné S, Nicolet C, Tsujimoto Y and Avellan F 2014 *Journal of Hydraulic Research* **52**(3) 399-411
[12] Alligné S, Landry C, Favrel A, Nicolet C, Avellan F 2015 *Journal of Physics: Conference Series* **656**(1) 012056
[13] Landry C, Favrel A, Müller A, Nicolet C and Avellan F 2016 *Journal of Hydraulic Research* **54**(2) 185-196
[14] Yamamoto K, Müller A, Favrel A and Avellan F 2017 *Experiments in Fluids* **58**(10) 142
[15] Favrel A, Müller A, LandryC, Yamamoto K and Avellan F 2015 *Experiments in Fluids* **56**(12) 215
[16] Müller A, Dreyer M, Andreini N and Avellan F 2013 *Experiments in Fluids* **54**(4) 1514
[17] Duparchy A, Guillozet J, De Colombel T and Bornard L 2014 *IOP Conference Series: Earth and Environmental Science* **22** 032016
[18] Favrel A, Gomes Pereira Junior J, Landry C, Müller A, Nicolet C and Avellan F 2018 *Journal of Hydraulic Research* **56**(3) 367-379
[19] Nicolet C 2007 *Hydroacoustic modelling and numerical simulation of unsteady operation of hydroelectric systems* Ph.D. thesis, EPFL, Lausanne, Switzerland
[20] Brennen C and Acosta A 1976 *Journal of Fluids Engineering, Transactions of the ASME,* **98** Ser 1(2)
[21] Favrel A, Gomes Pereira Junior J, Landry C, Alligné S, Andolfatto L, Nicolet C and Avellan F 2018 *Journal of Hydraulic Research* Under review
[22] Andolfatto L, Delgado J, Vagnoni E, Münch-Alligné C and Avellan F 2015 *E-Proceeding of the 36th IAHR World Congress 2015, La Hague, Netherlands*